Journal of Molecular Liquids 211 (2015) 742–746

Contents lists available at ScienceDirect

Journal of Molecular Liquids

journal homepage: www.elsevier.com/locate/molliq

# Effects of size and surface functionalization of zinc oxide (ZnO) particles on interactions with bovine serum albumin (BSA)

G. Simonelli [a,*], E.L. Arancibia [b]

[a] Laboratorio de Física del Sólido, Departamento de Física, FACET, Universidad Nacional de Tucumán, Av. Independencia 1800, T4002BLR S. M. Tucumán, Argentina
[b] INQUINOA-CONICET-UNT — Departamento de Ingeniería Procesos y Gestión Industrial, FACET, Universidad Nacional de Tucumán, Av. Independencia 1800, T4002BLR S. M. Tucumán, Argentina

ARTICLE INFO

*Article history:*
Received 29 December 2014
Received in revised form 30 July 2015
Accepted 31 July 2015
Available online xxxx

*Keywords:*
Zinc oxide
Surface curvature
3-mercaptopropionic acid
Bovine serum albumin
Fluorescence spectroscopy
Circular dichroism

ABSTRACT

In this work, the behavior of bovine serum albumin (BSA) interacting with zinc oxide (ZnO) particles functionalized with 3-mercaptopropionic acid (3-MPA) and without any coating has been investigated. Two kinds of ZnO particles of different size and morphology were obtained: microwires (MW) and nanoparticles (NP). The effect of surface modification on the fluorescence properties of ZnO was studied. Typical ZnO green emission due to defects was not observed in the functionalized NP spectrum. Structure alterations of the protein interacting with ZnO particles were evaluated by fluorescence spectroscopy and circular dichroism (CD). Though BSA structure was not significantly perturbed in any case, some conformational changes were observed for BSA interacting with not functionalized MW.



## 1. Introduction

Zinc oxide (ZnO) is being widely studied because of its interesting properties for technological applications. It is a wide gap semiconductor (3.37 eV) with a large exciton binding energy, it has intrinsic ultra violet (UV) photoluminescence and green emission due to defects, is piezoelectric and can be ferromagnetic if it is suitably doped [1]. In addition, it can be obtained in many different nanostructured morphologies [2], with conductivity sensitive to environmental gases [2,3] and antibacterial effects [4,5]. Due their size, ZnO nanostructures can be used to interact with biomolecules and cells, which makes them interesting for biological applications as biosensing [6–8], drug delivery [9,10] or fluorescence imaging [11,12]. For the latter application, semiconductor probes have better photostability than organic fluorophores [13].

However, adverse effects of nanoparticles (NP) are not well known. As ZnO is currently being used in cosmetic products or as food additive, ZnO nanoparticles should have low toxicity and good biocompatibility. Surface properties, as well as the size and shape of particles are very important for their biocompatibility [14–16]. Protein adsorption and surface modification of NP appear to reduce their cytotoxicity [17]. Particles in a wide range of sizes and morphologies are of biological interest. For instance, NP of diameters less than 10 nm penetrate normal tissues but particles in the range of a few hundreds of nm to a few μm can penetrate tumor vessels [18,19].

Surface functionalizations of ZnO nanostructures have been reported. In [20] a series mono or bifunctional linkers were bounded to ZnO nanotip films and studied by Fourier transform infrared spectroscopy (FTIR) and UV spectroscopy. It is concluded that a potentially useful bifunctional linker is 3-mercaptopropionic acid (3-MPA) since it binds ZnO by the COOH group, leaving the SH group available for further modifications. In [21] ZnO quantum dots were successfully covered with mercaptoacetic acid, as evidenced by the modification of their luminescence properties.

3-MPA was used in [11] to introduce thiol groups onto the surface of ZnO nanowires for further functionalization to be specifically targeted to cell surface receptors for imaging of cancer cells.

As for biomedical applications NP interact with proteins or other biomolecules it is necessary to assess the effect the NP produce on the protein. Serum albumin is one of the most abundant proteins in plasma and plays an important role in many physiological functions [22].

Bovine serum albumin (BSA) is a protein that consists of three intrinsic fluorophores: tryptophan (trp), tyrosine (tyr), and phenylalanine (phy). Conformational changes of the protein can be evaluated exploiting photoluminescence properties of trp and optical activity of secondary structure composition. In [23] it was reported that BSA retained most of its α-helical structure after conjugation with gold NP

*Abbreviations:* MW, ZnO microwires; NP, ZnO nanoparticles; 3-MPA, 3-mercaptopropionic acid; 3MPA–MW, ZnO microwires functionalized with 3-mercaptopropionic acid; 3MPA–NP, ZnO nanoparticles functionalized with 3-mercaptopropionic acid; PBS–K, phosphate buffer solution–potassium; BSA, bovine serum albumin.

* Corresponding author.
*E-mail addresses:* gsimonelli@herrera.unt.edu.ar (G. Simonelli), earancibia@herrera.unt.edu.ar (E.L. Arancibia).

http://dx.doi.org/10.1016/j.molliq.2015.07.075
0167-7322/

of 40 nm of diameter. Similar results were obtained for similar size ZnO NP in [24,25]. For ZnO NP of 7.5 nm of diameter, the formation of aggregates of BSA–ZnO NP induces some conformational modification of BSA [26]. In [27] very little alterations in the ellipticity values in BSA circular dichroism (CD) spectrum were found on binding to 6 nm diameter NP of ZnO functionalized with polyethyleneimine (PEI), suggesting only a minor change in the three-dimensional configuration of the protein. The conformational behavior of albumin on conjugation with NP is of great importance and needs further understanding before such complexes are used in biomedical applications. This behavior is influenced by the size, morphology and surface properties of the particles [28].

In this work we study photoluminescence properties and the interaction with BSA of two different kinds of ZnO particles: microwires and nanoparticles. Both of them are functionalized with 3-MPA and the effect of the surface modification on the mentioned properties is evaluated. To reach this goal, the particles were synthetized, functionalized and characterized by means of SEM, XRD, EDS, FTIR and fluorescence spectroscopy. To study the interaction with BSA both fluorescence spectroscopy and circular dichroism techniques were used.

## 2. Materials and method

### 2.1. Preparation of ZnO samples

Two different methods were used to obtain the ZnO samples:

#### 2.1.1. Microwires of ZnO (MW)

Microwires of ZnO (MW) were prepared by direct carbothermal growth [29]: a pellet mixture of ZnO (Puratronic® 99.9995% Alfa Aesar) and graphite (powder 99.9995% Alfa Aesar), mass ratio of 1:1 was introduced in a quartz tube inside a furnace at 1150 °C during 45 min in air and at atmosphere pressure. The wires grow directly on the pellet.

#### 2.1.2. ZnO nanoparticles (NP)

ZnO nanoparticles (NP) were obtained from a colloidal suspension prepared following the method described in [30]. Briefly, a 1 mM of zinc acetate dihydrate (99.5%) was dissolved in 80 ml 2-propanol (99.9%) at 50 °C and later diluted to 920 ml. 80 ml of a 0.02 M of sodium hydroxide (99.5%) solution in 2-propanol was then added at 0 °C within 1 min under continuous stirring. The mixture was immersed for 2 h into a water bath preheated to 65 °C. After three days of further aging at room temperature, the solvent was removed by rotary evaporation.

### 2.2. Functionalization

ZnO MW and NP were functionalized with 3-MPA as described in [11]: 3 mg of 3-MPA (Sigma Aldrich) were added to suspensions of 5 mg of MW and NP in 2 ml of dichloromethane (DCM) each. The reaction mixture was stirred at room temperature for 1 h. After evaporation of DCM, the white solid was collected and washed with ethanol three times.

### 2.3. BSA solutions

BSA fatty acid free was purchased from Aldrich and was directly used. We have used Millipore water for preparing solutions. BSA concentration was $2.10^{-6}$ M in PBS–K (pH = 6.8) and ZnO particles were added in the range of $6.10^{-6}$ M–$4.10^{-5}$ M.

### 2.4. Characterization

The morphology and composition of the samples before and after functionalization were characterized by Scanning Electron Microscopy (SEM) and Energy Dispersive Spectroscopy (EDS) (Carl Zeiss Supra 40). Crystal structures of the samples before functionalization were analyzed using X-ray diffraction (XRD) (Panalytical Empyrean with PIXcel 3D detector, high stability Cu source). The infrared absorption spectrum was recorded in KBr using a Perkin–Elmer GX FTIR instrument. An F-2500 Hitachi spectrofluorometer was used for fluorescence spectroscopy. Circular dichroism (CD) has been recorded by JASCO, CD spectrometer, model J-815 using a 1 cm path length. All experiments were performed at room temperature.

## 3. Results

### 3.1. Characterization of bare and functionalized MW and NP

High crystalline MW and uniform size NP were obtained, as shown in figure S1 (Supporting Information). MW have diameters between

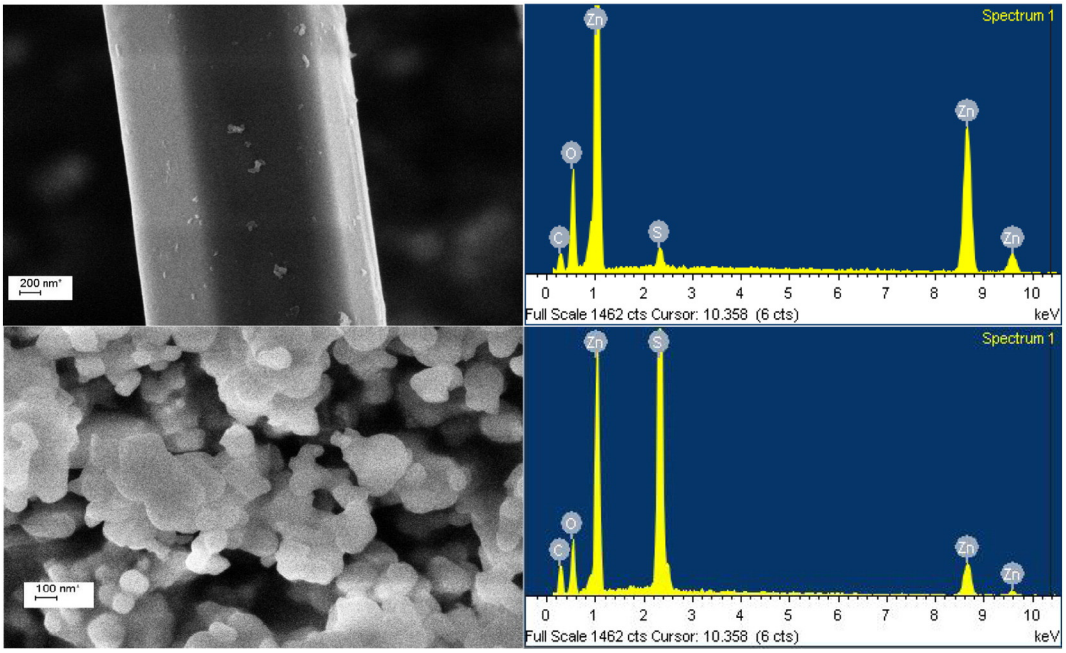


**Fig. 1.** Left: SEM images of ZnO 3MPA–MW (top) and 3MPA–NP (bottom). Right: corresponding EDS spectra.

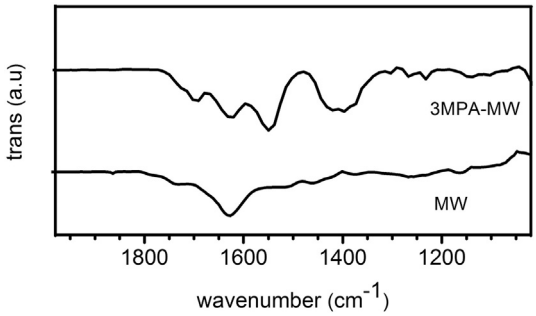


**Fig. 2.** Detail of FTIR spectra of MW and 3MPA–MW in the range of 1000–2000 $cm^{-1}$ taken from spectra performed between 400 and 4000 $cm^{-1}$.

0.5–5 μm and length of some hundreds of μm. NP have a diameter 30 nm. X-ray diffraction patterns in figure S2 (Supporting Information) correspond to a high crystalline wurzite structure of MW and present not so well defined peaks for the NP. After functionalization, MW and NP did not change their morphology. SEM images are presented in Fig. 1. In that figure, EDS spectra of the functionalized samples are also presented. In both samples, the presence of sulfur from the 3-MPA is detected. However, it is suggested from the figure that the coverage of MW with 3-MPA is less effective than for NP.

FTIR spectra were performed in the range of 400–4000 $cm^{-1}$. In all samples, –OH stretching band at 3300–3600 $cm^{-1}$ and ZnO band at 460 $cm^{-1}$ were observed. For clarity, in Fig. 2 only the spectra in the range of 1000–2000 $cm^{-1}$ of MW and functionalized MW are presented. In this figure, for both samples a band at 1633 $cm^{-1}$ is observed which can be attributed to δO–H bending of sample moisture as observed in other reports [31]. For the functionalized MW sample, a peak is found at 1700 $cm^{-1}$ corresponding to the characteristic peak of C═O group from the 3-MPA which in our case does not disappear completely. In addition, important peaks are observed at 1551 $cm^{-1}$ and at 1420 $cm^{-1}$ which are assigned to the antisymmetric and symmetric stretching of the carboxylate group ($COO^-$) [20,32]. These results suggest that the binding of 3-MPA to ZnO occurs preferentially by formation of surface bonds by the COOH group rather than through the SH group, in accordance with [20].

Photoluminescence spectra of bare and functionalized MW and NP are presented in Fig. 3. These spectra were obtained as a juxtaposition of emission spectra for $\lambda \geq 410$ nm and excitation spectra for $\lambda < 410$ nm. It is seen that both MW and NP without functionalization show the two characteristic ZnO peaks [1]: one in the UV range due to the exciton and the other in the visible range due to defects, with maximum at 520 nm (MW) and 550 nm (NP). In the case of MW, there are no qualitative changes in the photoluminescence spectrum before and after functionalization with 3-MPA. In the case of NP there are major changes in the spectrum after functionalization: the UV peak is shifted right and the green luminescence due to defects completely disappears. In this case, 3-MPA coating of the particles is complete and quenches the defect emission. Surface oxygen vacancies or, equivalently, excess $Zn^{2+}$ are the main responsible of green emission for particles with a high surface/volume relationship. The effect of the 3-MPA is the passivation of the dangling bonds of these defect states, as polyvinyl-alcohol does in [33]. In our case, passivation can be explained by the binding of the 3-MPA molecule to the NP through its carboxyl group, which occupies the oxygen defects at the surface of ZnO nanoparticles as reported in [34] for amphoteric surfactant molecules. Passivation effects must be taken into account if ZnO is intended to be used for fluorescence imaging.

### 3.2. Interaction with BSA

In order to study the interaction between ZnO and BSA, and 3-MPA functionalized ZnO and BSA, the quenching of fluorescence of a solution of BSA with the addition of ZnO particles was investigated. The effects of the addition of MW and functionalized MW to a $2.10^{-6}$ M solution of BSA are shown in Fig. 4 a) and b), respectively.

Tryptophan residues of BSA are responsible of its fluorescence. BSA has two tryptophan residues: trp-212, located within a hydrophobic cavity and trp-134 on the surface of the molecule. Fig. 4 clearly shows that the BSA has a strong emission band at 339 nm when excited with 280 nm wavelength. The intensity of the fluorescence band decreases with increasing concentration of ZnO MW and functionalized ZnO MW, though the effect is stronger for bare ZnO MW. The quenching of the BSA fluorescence is due to a static type of quenching mechanism: the formation of a non-fluorescent ground state complex which perturbs the fluorophore environment, as reported in [24,26,35]. 3-MPA is a short linker and it may not shield completely the BSA from ZnO but, as the overall quenching is less for the functionalized MW, it is inferred that the interaction BSA-3MPA does not affect the tryptophan environment as much as the direct interaction BSA-ZnO.

CD spectroscopy evaluates conformational changes in protein on binding to nanoparticle, so it gives further insight into protein-particle interaction. In Fig. 5, CD spectra of a $2.10^{-6}$ M solution of BSA with the addition of ZnO MW and 3MPA–MW are shown. It is seen that there are two strong negative bands in the UV region at 209 and 221 nm [36], which are characteristic of the α-helical structure of the protein. The addition of particles causes a small reduction of the observed signal, indicating some decrease in the α-helical structure content. Results for ZnO MW are consistent with other reports [24,26], being the decrease in α-helical structure content not significant and, therefore, the structure of the protein in both cases is virtually preserved. Notice that the reduction of the observed signal is greater for not functionalized ZnO particles. CD spectra for BSA with ZnO NP and 3MPA–NP (not shown) did not give any significant reduction of BSA signal.

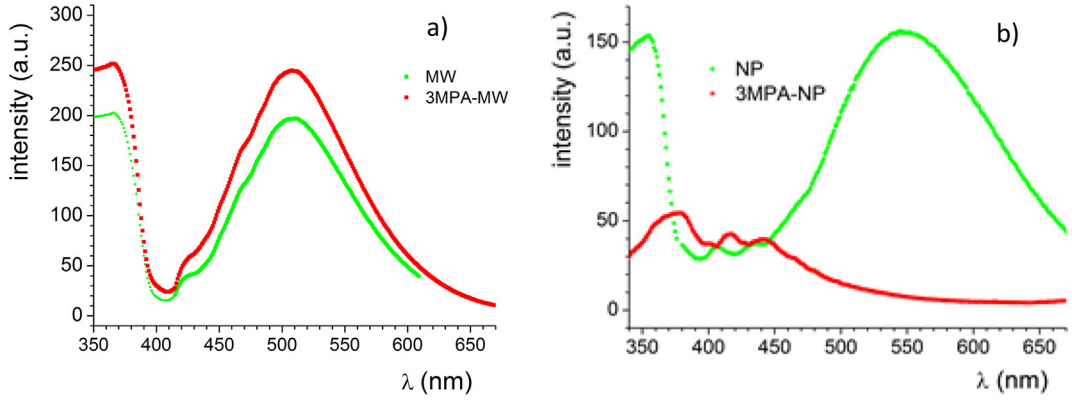


**Fig. 3.** a) Photoluminescence spectrum of MW and 3MPA–MW. Emission spectrum excited with 370 nm and excitation spectrum at 510 nm. b) Photoluminescence spectrum of NP and 3MPA–NP. Emission spectrum excited with 350 nm and excitation spectrum at 545 nm.

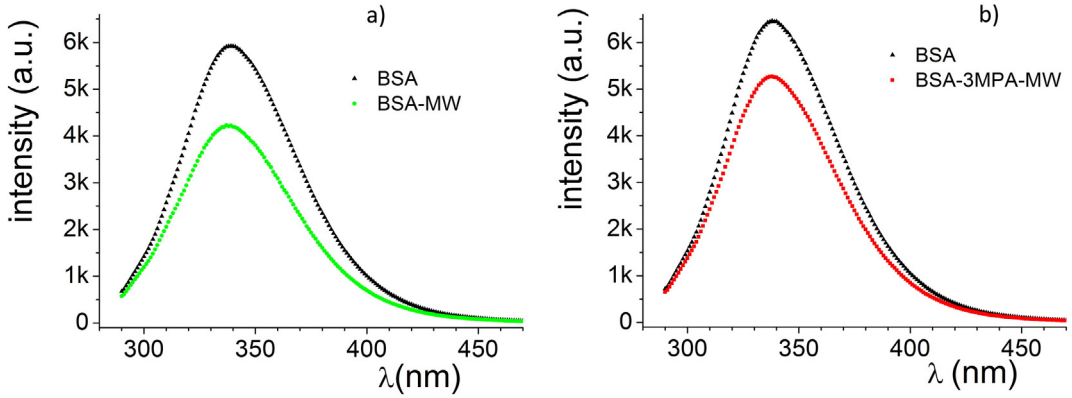


**Fig. 4.** a) Fluorescence spectra of BSA solution $2.10^{-6}$ M in PBS–K (pH = 6.8) and BSA with the addition of ZnO MW 3.5 $10^{-5}$ M (maximum concentration of ZnO particles, intermediate concentrations are not shown), $\lambda_{exc}$ = 280 nm. b) Same as a) for 3MPA–MW 3.5 $10^{-5}$ M.

It is known that the structure of proteins can be affected when they are adsorbed on nanoparticles. The size of the particles and their surface curvature, are key issues in the structure alteration, as well as the type of protein involved: globular or fibrillar [37]. BSA, being a globular protein, tends to maintain its structure when adsorbed on highly curved surfaces, preserving its functional properties [38,39]. This effect can be explained by a simple model: flat surfaces exhibit more contact area for adsorbed proteins, according to the side-on model for BSA [40]. Therefore, a stronger interaction between protein and nanoparticle results and the perturbation of the protein structure is more important. Our results indicate that the higher curvature of NP surface with respect to MW is responsible for the differences in the CD spectrum.

Interestingly, comparing the CD spectra of BSA with ZnO MW and 3MPA–MW, a more important perturbation of the protein structure is obtained for the former case, for functionalized MW only marginal perturbation is perceived. This can be explained considering that for bare MW, BSA is in direct contact with $Zn^{2+}$ and $-O^{-}$, after displacing water molecules. In the other hand, for the functionalized MW, BSA is anchored by hydrogen bonds between –SH and different possible connection points of BSA. Similarly, some differences in interactions between BSA and ZnO nanoparticles and BSA and polyethyleneimine-functionalized ZnO nanoparticles were reported in [27].

## 4. Conclusions

High crystalline MW were obtained, with diameters between 0.5–5 μm and length of some hundreds of μm and uniform size NP were obtained with diameter 30 nm. After functionalization, MW and NP did not change their morphology. FTIR results suggest that the binding of 3-MPA to ZnO occurs preferentially by formation of surface bonds by the COOH group rather than through the SH group.

Photoluminescence studies of bare and functionalized MW and NP show that in the case of NP, for which the surface coverage with 3-MPA is greater than for MW, green luminescence disappears with functionalization due to the passivation of ZnO surface dangling bonds.

Fluorescence spectroscopy of BSA with MW and 3MPA–MW indicates that tryptophan emission is less affected for functionalized particles. DC spectra indicate that aggregates of BSA with ZnO MW induce minor conformational changes in BSA. On the other hand, neither 3MPA–MW nor NP or 3MPA–NP induces any significant change in BSA DC spectrum. This is consistent with our photoluminescence results, in the sense that functionalization tends to preserve the protein structure. In addition, the higher curvature of NP surface with respect to MW is responsible for the preservation of the protein structure interacting with NP.

Therefore, our results indicate that overall, BSA structure is preserved when interacting with ZnO particles. However surface properties and size of particles are determinant of these interactions and could be tailored to enhance biocompatibility of the particles.

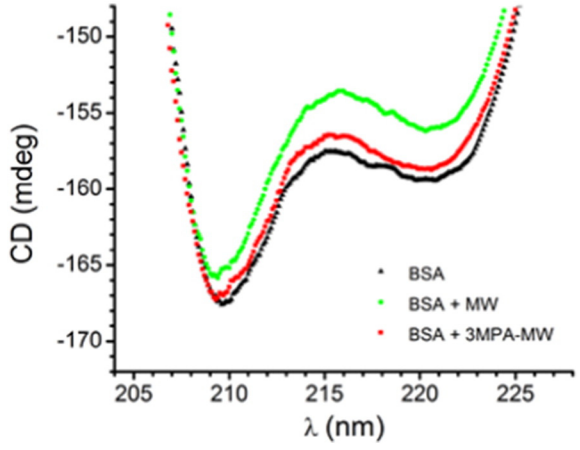


**Fig. 5.** CD spectra of BSA solution $2.10^{-6}$ M in PBS–K (pH = 6.8) and BSA with the addition of ZnO MW 3.5 $10^{-5}$ M and same concentration of 3MPA–MW.

## Acknowledgments

This work was partially sponsored by CIUNT (Consejo de Investigaciones de la Universidad Nacional de Tucumán) and partially by PICT 10–14560 of ANPCyT (Agencia Nacional de Promoción Científica y Tecnológica). E.L.A. is a member of CONICET (Consejo Nacional de Investigaciones Científicas y Técnicas de la República Argentina).

## Appendix A. Supplementary data

Supplementary data to this article can be found online at http://dx.doi.org/10.1016/j.molliq.2015.07.075.

## References

[1] H. Morkoç, U. Özg€ur, Zinc oxide: fundamentals, materials and device technology Wiley-VCH, Verlag GmbH & Co. KGaA, Weinheim, 2009.
[2] Z.L. Wang, Zinc oxide nanostructures: growth, properties and applications, J. Phys. Condens. Matter 16 (2004) R829–R858.
[3] M.-W. Ahn, K.-S. Park, J.-H. Heo, J.-G. Park, D.-W. Kim, K.J. Choi, J.-H. Lee, S.-H. Hong, Gas sensing properties of defect-controlled ZnO-nanowire gas sensor, Appl. Phys. Lett. 93 (2008) 1–3 (263103).
[4] N. Padmavathy, R. Vijayaraghavan, Enhanced bioactivity of ZnO nanoparticles—an antimicrobial study, Sci. Technol. Adv. Mater. 9 (2008) 1–7 (035004).
[5] T. Gordona, B. Perlstein, O. Houbara, I. Felner, E. Banin, S. Margel, Synthesis and characterization of zinc/iron oxide composite nanoparticles and their antibacterial properties, Colloids Surf. A Physicochem. Eng. Asp. 374 (2011) 1–8.

[6] S.K. Arya, S. Saha, J.E. Ramirez-Vick, V. Gupta, S. Bhansali, S.P. Singh, Recent advances in ZnO nanostructures and thin films for biosensor applications: Review, Anal. Chim. Acta 737 (2012) 1–21.
[7] J. Kim, S. Kwon, J.K. Park, I. Park, Quantum dot-based immunoassay enhanced by high-density vertical ZnO nanowire array, Biosens. Bioelectron. 55 (2014) 209–215.
[8] Y. Cao, E. Galoppini, P. Ivanoff Reyes, Z. Duan, Y. Lu, Morphology effects on the biofunctionalization of nanostructured ZnO, Langmuir 28 (2012) 7947–7951.
[9] Y. Zhang, H.F. Chan, K.W. Leong, Advanced materials and processing for drug delivery: The past and the future, Adv. Drug Deliv. Rev. 65 (2013) 104–120.
[10] Y. Chen, L. Liu, Modern methods for delivery of drugs across the blood–brain barrier, Adv. Drug Deliv. Rev. 64 (2012) 640–665.
[11] H. Hong, J. Shi, Y. Yang, Y. Zhang, J.W. Engle, J. Nickles, X. Wang, W. Cai, Cancer-targeted optical imaging with fluorescent zinc oxide nanowires, Nano Lett. 11 (2011) 3744–3750.
[12] Sheng-Chieh Yang, Yi-Chun Shen, Tzu-Chun Lu, Tsung-Lin Yang, Jian-Jang Huang, Tumor detection strategy using ZnO light-emitting nanoprobes, Nanotechnology 23 (2012) 1–6 (055202).
[13] Changxia Sun, Jinghe Yang, Lei Li, Xia Wu, Liu Yang, Shufang Liu, Advances in the study of luminescence probes for proteins, J. Chromatogr. B 803 (2004) 173–190.
[14] H. Yin, P.S. Casey, M.J. McCall, M. Fenech, Effects of surface chemistry on cytotoxicity, genotoxicity, and the generation of reactive oxygen species induced by ZnO nanoparticles, Langmuir 26 (2010) 15399–15408.
[15] T.W. Prow, J.E. Grice, L.L. Lin, R. Faye, M. Butler, W. Becker, E.M.T. Wurm, C. Yoong, T.A. Robertson, H.P. Soyer, M.S. Roberts, Nanoparticles and microparticles for skin drug delivery, Adv. Drug Deliv. Rev. 63 (2011) 470–491.
[16] L. Shia, J. Shan, Y. Ju, P. Aikens, R.K. Prud'homme, Nanoparticles as delivery vehicles for sunscreen agents, Colloids Surf. A Physicochem. Eng. Asp. 396 (2012) 122–129.
[17] D. Bartczak, M.-O. Baradez, S. Merson, H. Goenaga-Infante, D. Marshall, J. Phys. Conf. Ser. 429 (2013) 1–7 (012015).
[18] J.H. Grossman, S.E. McNeil, Nanotechnology in cancer medicine, Phys. Today 65 (2012) 38–42.
[19] S.K. Hobbs, W.L. Monsky, F. Yuan, W.G. Roberts, L. Griffith, V.P. Torchilin, R.S. Jain, Regulation of transport pathways in tumor vessels: role of tumor type and microenvironment, Proc. Natl. Acad. Sci. U. S. A. 95 (1998) 4607–4612.
[20] O. Taratula, E. Galoppini, D. Wang, D. Chu, Z. Zhang, H. Chen, G. Saraf, Y. Lu, Binding of molecular linkers to ZnO and MgZnO nanotip films, J. Phys. Chem. B 110 (2006) 6506–6515.
[21] R. Song, Y. Liu, L. He, Synthesis and characterization of mercaptoacetic acid-modified ZnO nanoparticles, Solid State Sci. 10 (2008) 1563–1567.
[22] X.M. He, D.C. Carter, Atomic structure and chemistry of human serum albumin, Nature 358 (1992) 209–215.
[23] N. Wangoo, C. Raman Suri, C. Shekhawat, Interaction of gold nanoparticles with protein: a spectroscopic study to monitor protein conformational changes, Appl. Phys. Lett. 92 (2008) 1–3 (133104).
[24] M. Bardhan, G. Mandal, T. Ganguly, Steady state, time resolved, and circular dichroism spectroscopic studies to reveal the nature of interactions of zinc oxide nanoparticles with transport protein bovine serum albumin and to monitor the possible protein conformational changes, J. Appl. Phys. 106 (2009) 1–5 (034701).
[25] U. Dembereldorj, E.-O. Ganbold, J.-H. Seo, S.Y. Lee, S.I. Yang, S.-W. Joo, Conformational changes of proteins adsorbed onto ZnO nanoparticle surfaces investigated by concentration-dependent infrared spectroscopy, Vib. Spectrosc. 59 (2012) 23–28.
[26] A. Bhogale, N. Patel, P. Sarpotdar, J. Mariam, P.M. Dongre, A. Miotello, D.C. Kothari, Systematic investigation on the interaction of bovine serum albumin with ZnO nanoparticles using fluorescence spectroscopy, Colloids Surf. B: Biointerfaces 102 (2013) 257–264.
[27] S. Chakraborti, P. Joshi, D. Chakravarty, V. Shanker, Z.A. Ansari, S.P. Singh, P. Chakrabarti, Interaction of polyethyleneimine-functionalized ZnO nanoparticles with bovine serum albumin, Langmuir 28 (2012) 11142–11152.
[28] A.A. Shemetov, I. Nabiev, A. Sukhanova, Molecular interaction of proteins and peptides with nanoparticles, ACS Nano 6 (2012) 4585–4602.
[29] B.Q. Cao, M. Lorenz, M. Brandt, H. von Wenckstern, J. Lenzner, G. Biehne, M. Grundmann, P-type conducting ZnO:P microwires prepared by direct carbothermal growth, Phys. Status Solidi (RRL) 2 (2008) 37–39.
[30] D.W. Bahnemann, C. Kormann, M. Hoffmann, Preparation and characterization of quantum size zinc oxide: a detailed spectroscopy study, J. Phys. Chem. 91 (1987) 3789–3798.
[31] B. Zhang, T. Kong, W. Xu, R. Su, Y. Gao, G. Cheng, Surface functionalization of zinc oxide by carboxyalkylphosphonic acid, self-assembled monolayers, Langmuir 26 (2010) 4514–4522.
[32] T. Burks, M. Avila, F. Akhtar, M. Göthelid, P.C. Lansåker, M.S. Toprak, M. Muhammed, A. Uheida, Studies on the adsorption of chromium(VI) onto 3-mercaptopropionic acid coated super paramagnetic iron oxide nanoparticles, J. Colloid Interface Sci. 425 (2014) 36–43.
[33] L. Qin, C. Shing, S. Sawyer, P.S. Dutta, Enhanced ultraviolet sensitivity of zinc oxide nanoparticle photoconductors by surface passivation, Opt. Mater. 33 (2011) 359–362.
[34] H. Usui, Y. Shimizu, T. Sasaki, N. Koshizaki, Photoluminescence of ZnO nanoparticles prepared by laser ablation in different surfactant solutions, J. Phys. Chem. B 109 (2005) 120–124.
[35] A. Kathiravan, G. Paramaguru, R. Renganathan, Study on the binding of colloidal zinc oxide nanoparticles with bovine serum albumin, J. Mol. Struct. 934 (2009) 129–137.
[36] Y.-Z. Zhang, B. Zhou, Y.-X. Liu, C.-X. Zhou, X.-L. Ding, Y. Liu, Fluorescence study on the interaction of bovine serum albumin with P-aminoazobenzene, J. Fluoresc. 18 (2008) 109–118.
[37] M. Lundqvist, J. Stigler, G. Elia, I. Lynch, T. Cedervall, K.A. Dawson, Nanoparticle size and surface properties determine the protein corona with possible implications for biological impacts, Proc. Natl. Acad. Sci. U. S. A. 105 (2008) 14265–14270.
[38] P. Roach, D. Farrar, C.C. Perry, Surface tailoring for controlled protein adsorption: effect of topography at the nanometer scale and chemistry, J. Am. Chem. Soc. 128 (2006) 3939–3945.
[39] J.H. Teichroeb, J.A. Forrest, V. Ngai, L.W. Jones, Anomalous thermal denaturing of proteins adsorbed to nanoparticles, Phys. J. E 21 (2006) 19–24.
[40] S.T.J. Su, J.R. Lu, R.K. Thomas, Z.F. Cui, Effect of pH on the adsorption of bovine serum albumin at the silica/water interface studied by neutron reflection, J. Phys. Chem. B 103 (1999) 3727–3736.